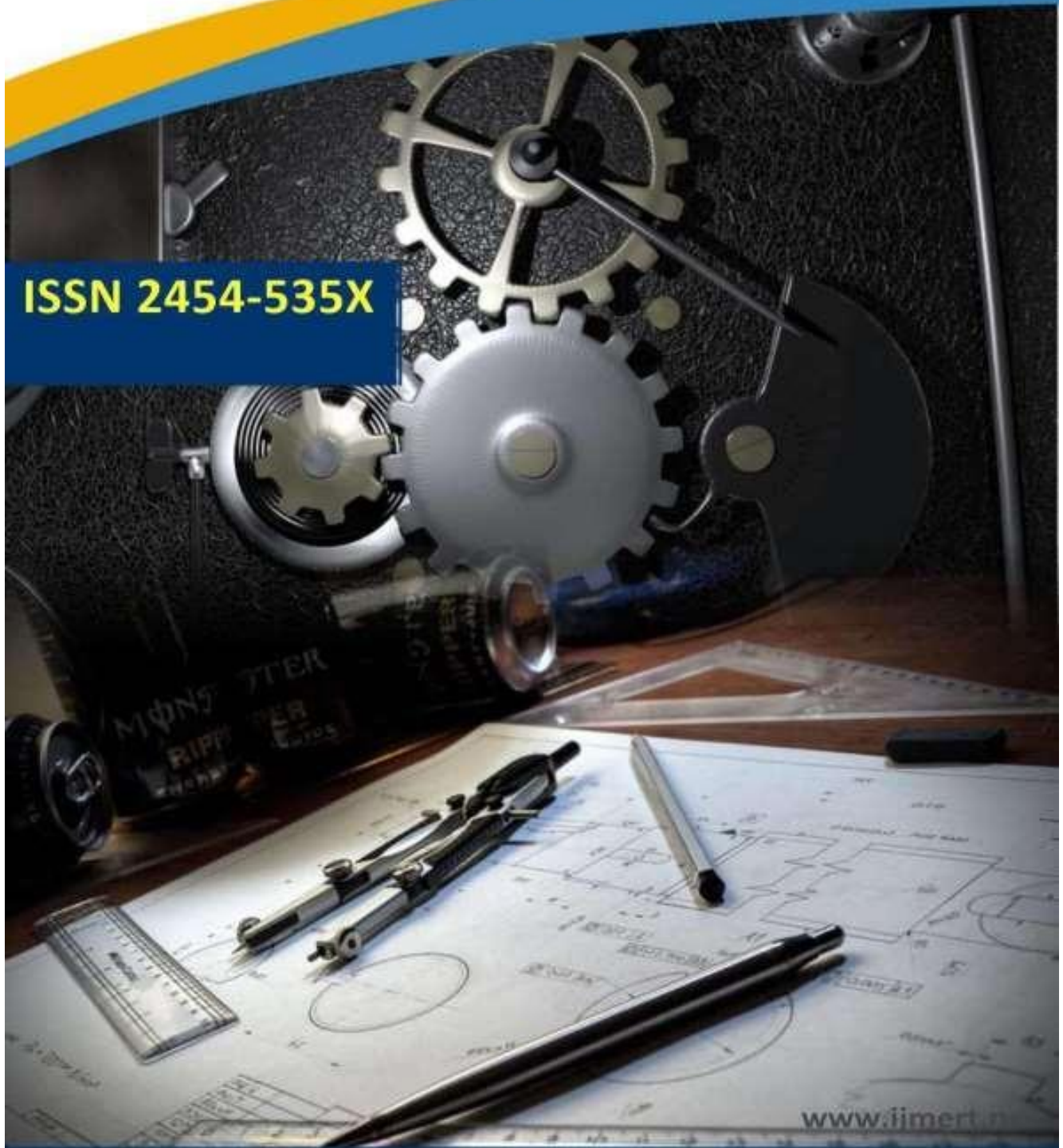




International Journal of Mechanical Engineering Research and Technology

ISSN 2454-535X



Email ID: info.ijmert@gmail.com or editor@ijmert.net



Study on Coaxial Thermoacoustic System Resonance Control by Locally Expanding The Outer Tube.

Rakesh, Santosh, Yeshwanth, Dayakar, Yeshwanth, and Yashodhar

[†]Faculty of Science and Engineering, Doshisha University 1-3 Tataramiyakodani, Kyotanabe, Kyoto 610-0321, Japan

[‡]School of Engineering, University of Shiga Prefecture 2500 Yasaka, Hikone, Shiga 522-8533, Japan

^{††}Facility of Biomedical Information, Doshisha University 1-3 Tataramiyakodani, Kyotanabe, Kyoto 610-0321, Japan

*Corresponding Author Email: sst0367@mail4.doshisha.ac.jp

ABSTRACT:

The regulation of the sound field in the tube, specifically that of the resonance mode, is researched in order to improve the cooling capacity of a coaxial-type thermoacoustic system. The coaxial type thermoacoustic system, which consists of two tubes with different radii, has the ability to create a traveling wave sound field with a high energy conversion efficiency. Additionally, this technology is suitable for downsizing due to its linear design. The prime mover's (PM) setting position, however, differs from the loop-tube kind. The fundamental mode's sound pressure is improved and the range of the cooling ability rises as the setting location is shifted closer to the tube end.

INTRODUCTION

Environmental problems including air pollution and global warming have gotten much worse in recent years. Then, all the focus is on a thermoacoustic system. A thermoacoustic system is one that uses the mutual transfer of heat and sound known as the thermoacoustic phenomena. [1-6] A sound wave oscillates by creating a steep temperature difference between both ends of a device called a stack's many tiny tubes. Since this system uses an external combustion engine, it can be powered by

The experimental system is illustrated in Figure 1. A stainless steel tube with a 42 mm inner diameter and a 2100 mm total length is used for the outer tube closed at both ends. A coordinate whose origin ($x = 0$) is set at the left end of the outer tube is defined. Another stainless tube with a 27 mm outer diameter, a 2000 mm total length and a 1 mm thickness is used for the inner tube open at both ends. The inner tube is set in the range $50 \text{ mm} \leq x \leq 2050 \text{ mm}$ coaxially with the outer tube. Air of atmospheric pressure is encapsulated in the tube. A stack made from a honeycomb ceramic with a 50 mm length and a 0.65 mm flow-path radius is used for PM. PM is set so that the position of the normal temperature end where 20°C water is circulated is $x_{PM} = 1700 \text{ mm}$. On the other hand, an electric heater is installed at the high temperature end of PM and a 330 W electric power is supplied. In order to suppress the shift of the resonance mode, attention is paid to the distribution of the sound pressure formed in an annular flow path (the flow path in the outer tube). The sound pressure distribution at the secondary mode formed in the annular flow path is illustrated in Figure 2. By expanding the radius of the outer tube in the range $990 \text{ mm} \leq x \leq 1040 \text{ mm}$ for the acoustical boundary condition for suppressing the secondary mode, the condition that the node easily

solar energy and factory exhaust heat. [7-9] Furthermore, it requires minimal maintenance because there are no mechanical moving parts. There are two types of thermoacoustic systems: standing-wave type and traveling-wave type. Since the traveling-wave type performs the energy conversion during the traveling-wave phase,

EXPERIMENTAL METHOD

appears there is furnished. This position is the location for the antinode of the secondary mode. Since the condition that the node easily appears at the position of the antinode is provided, the reduction of the secondary mode is expected. The inner diameter x_{ID} of the expanded outer tube is changed from 42 mm (before the expansion) to 60, 80 and 100 mm. At each size, the sound pressure in the annular flow path is measured with a pressure sensor (product of PCB Co.) after making sure the temperatures at both ends of PM have been reached at the steady state. [16]

: Circulating water: Heater: Stack

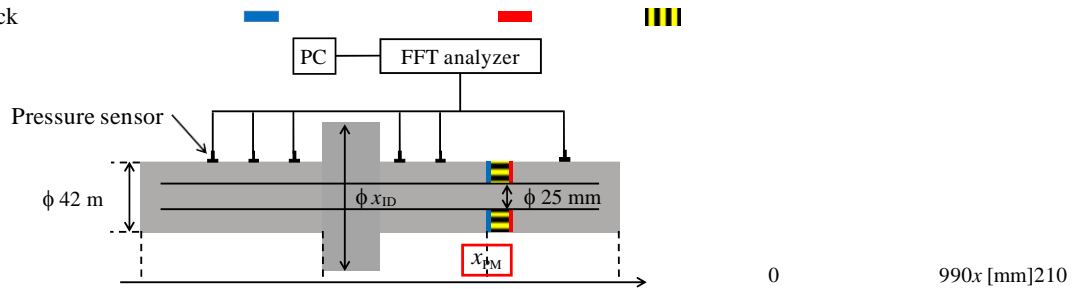
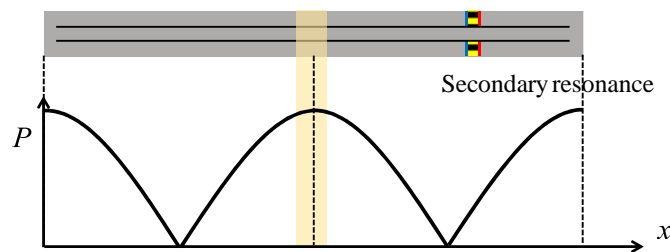


Figure 1. Experimental setup

Figure 2. Schematic of the sound pressure distribution in the annular area.

EXPERIMENTAL RESULTS AND DISCUSSION



In each value of x_{ID} , the sound wave with a wavelength of total flow path length is confirmed to be excited. Examples of the spectrum observed at $x = 120$ mm with $x_{ID} = 42$ mm (before the expansion) is shown in Figure 3 and with $x_{ID} = 100$ mm is shown in Figure 4. Increasing the level difference between the fundamental mode and secondary mode is confirmed with the expanded tube. To confirm the suppression effect of the second mode by increasing x_{ID} , the level difference between the fundamental mode and the secondary mode observed at $x = 120$ mm is shown in Figure 5. Since the sound level difference between the fundamental mode and the secondary mode increases with x_{ID} , it is seen that the expansion of the outer radius of the annular flow path is effective for the suppression of the second mode. The reason is discussed from the view point of the sound pressure distribution in the annular flow path. When the radius of the outer tube is expanded, the boundary condition to have the node of each mode easily appear at the expanded position is provided. Since the vicinity of the center of the tube is expanded in this experiment, it is the boundary condition that the center of the tube easily becomes the node. The schematic of the sound pressure distribution formed in the annular flow path is shown in Figure 6. Figure 6 (a) shows the pressure distribution of the fundamental mode and Figure 6 (b) shows the secondary mode whose suppression is attempted here. When the boundary condition to make the center of the tube ready to set the node is provided, the condition that the secondary mode as shown in Figure 6 (c) is easily excited is obtained. However, since the gradient of this sound pressure distribution does not agree with the gradient of the pressure distribution of the fundamental mode at the PM setting position, the oscillation of this second mode is hardly excited. Then the resonance shift to the secondary mode turns to be suppressed. An example of the sound pressure distribution in the fundamental mode formed in the annular flow path of $x_{ID} = 60$ mm is shown in Figure 7. From this figure, the fundamental mode can be confirmed to have the sound pressure distribution with a node at the center of the tube. Since the boundary condition to facilitate the appearance of the sound pressure node is provided at the position of the node of the sound pressure of the fundamental mode, the fundamental mode is scarcely affected by the boundary condition, and then it is supposed that the difference in the sound pressure level between the fundamental frequency component and the second harmonic frequency component is enhanced.

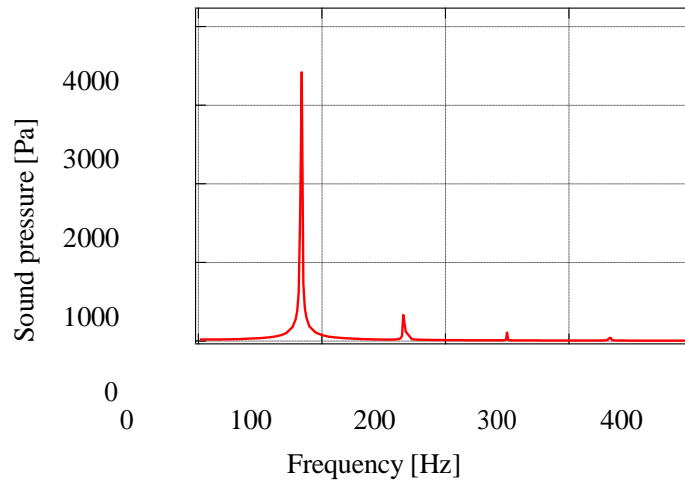


Figure 3. Frequency spectrum with $x_{ID} = 42$ mm

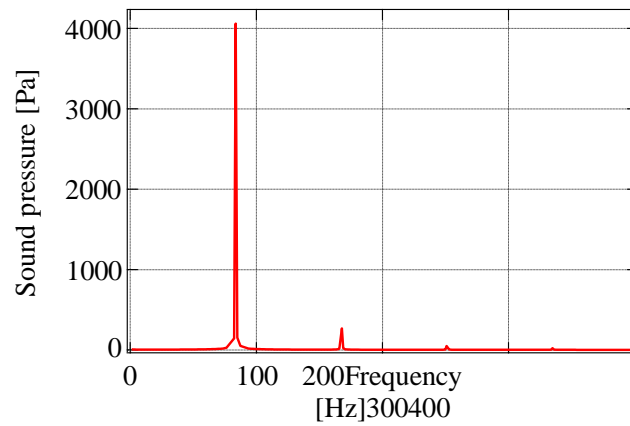


Figure 4. Frequency spectrum with $x_{ID} = 100$ mm



The sound pressure at $x = 50$ mm (the assumed setting position of HP) for various x_{ID} is shown in Figure 6. Comparing with the system with a uniform outer-tube radius of $x_{ID} = 42$ mm, the enhanced sound pressure is confirmed in the system of $x_{ID} = 60$ and 80 mm. However, in the system of $x_{ID} = 100$ mm, the sound pressure turns down comparing with the system of a uniform outer-tube radius. To investigate this reason, the attention is paid to the thickness of the viscous boundary layer of the high temperature end of PM. The thickness of the viscous boundary layer δ_v is defined as Eq. (1) $2\nu\delta_v = \sqrt{(1)}$ Working fluid in the viscous boundary layer does not contribute to the conversion between heat and sound. Using the temperature of the high temperature end of PM for various x_{ID} , the thickness of the viscous boundary layer δ_v is shown in Figure 7. The thickness of the viscous boundary layer δ_v is confirmed to be reduced in the cases of $x_{ID} = 60$ and 80 mm where the sound pressure is enhanced. This thickness of the viscous boundary layer δ_v reducing is assumed to take place because the energy conversion from heat to sound is more activated. On the other hand, in the case of $x_{ID} = 100$ mm, the thickness of the viscous boundary layer δ_v at the high temperature end is elevated compared to the system of uniform radius. Although the thermal input is concentrated to the fundamental mode because the secondary mode decreases, since the boundary condition designed in this experiment turns to be the condition that the working fluid is hard to exchange energy from heat to sound, the conversion efficiency from heat to sound lowers. Therefore it is seen that the optimum expanded radius exists between $x_{ID} = 80$ mm and $x_{ID} = 100$ mm.

SUMMARY

In the present paper, to suppress the shift of the fundamental resonance mode to the second mode that caused the degradation of the cooling effect, the control of the resonance mode was investigated by the technique to provide additional boundary condition. As the result, the suppression of the second mode generation was successfully performed and the promotion of the energy conversion from heat to sound resulted in the enhanced sound pressure of the fundamental mode. However, it was suggested that extreme boundary conditions could suppress not only the second mode but also the fundamental mode.

ACKNOWLEDGMENTS

This work was partly supported by JSPS grants-in-aid for young scientists (A) and (B), JSPS grant-in-aid for challenging exploratory research, grant-in-aid for scientific research (C), program for fostering regional innovation and JST super cluster program.

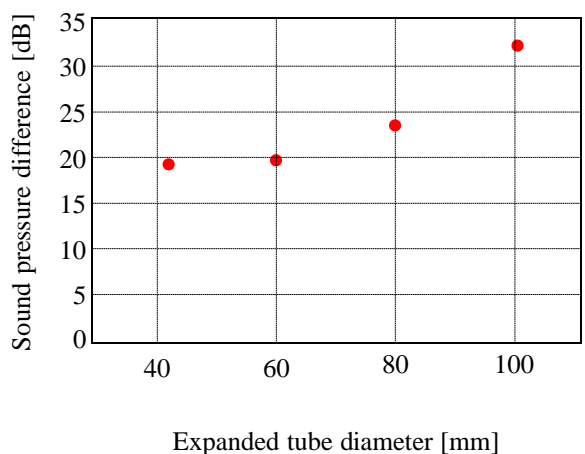


Figure 5. Difference of sound pressure level between fundamental and second mode components.

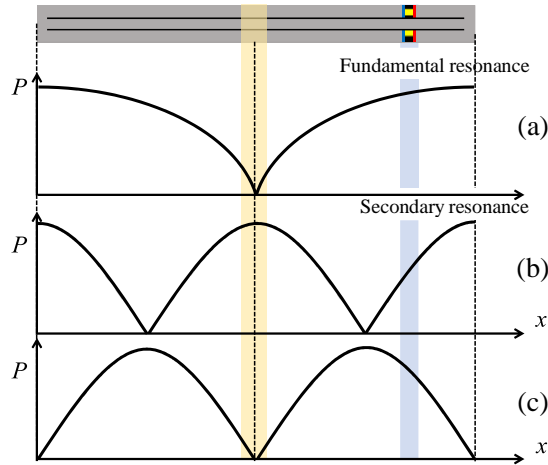
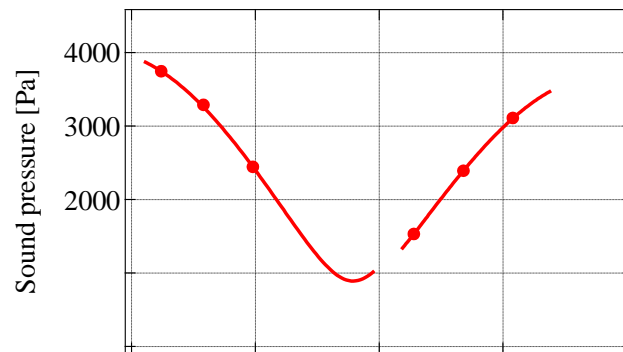


Figure 6. Schematic of fundamental and second mode sound pressure distributions in the annular area.



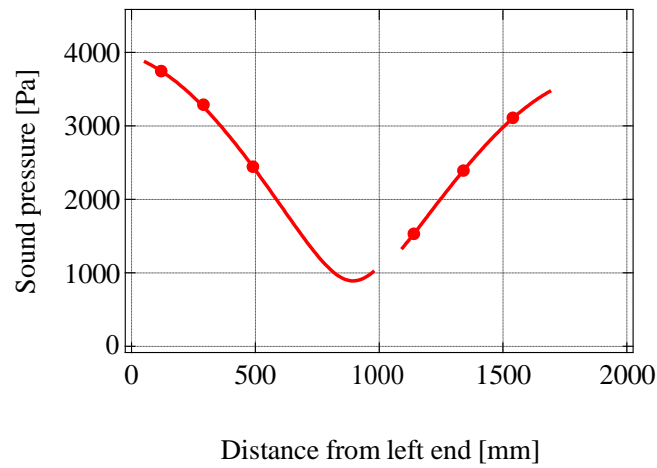


Figure 7. Distribution of sound pressure.

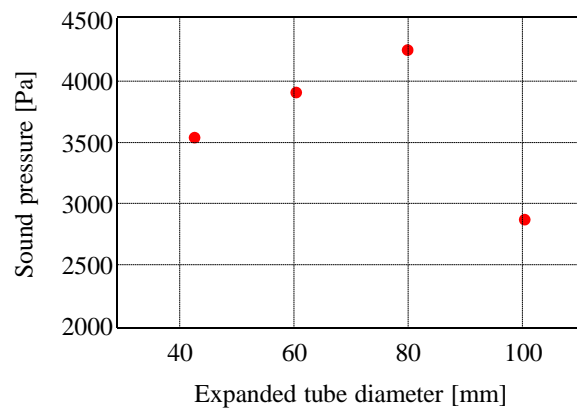


Figure 8. Relationship between expanded tube diameter and sound pressure.

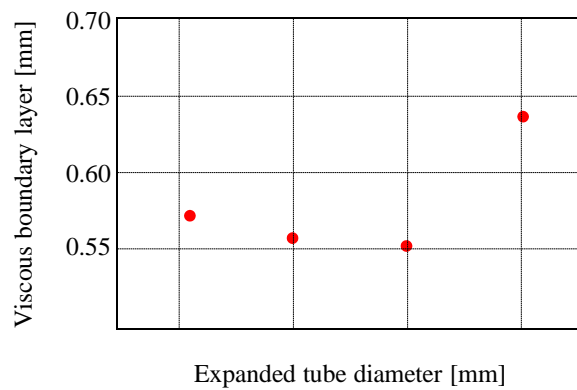


Figure 9. Relationship between expanded tube diameter and viscous boundary layer.



REFERENCES

- [1] P. H. Ceperley, "A pistonless Stirling engine—The traveling wave heat engine," *J. Acoust. Soc. Am.* vol. 66, no. 5, pp.1508- 1513, 1979.
- [2] G. W. Swift, "Thermoacoustic engines," *J. Acoust. Soc. Am.* vol. 84, pp. 1145, 1988.
- [3] W. Tianlei, "Nonlinear Control Strategies And Planning For Underactuated Overhead Cranes", *Engineering Heritage Journal*, vol. 3, no. 1, pp. 9-12, 2019.
- [4] S. Backhaus, and G. W. Swift, "A thermoacoustic Stirling heat engine," *Nature*, 339, pp. 335 -338, 1999.
- [5] T. Yazaki, A. Iwata, T. Maekawa, and A. Tominaga, "Traveling wave thermoacoustic engine in a looped tube," *Phys. Rev.Lett.*, vol.81, no.15, pp.3128-3131, 1998.
- [6] S. Sathishkumar, M. Kanna, "Topology Optimization Of Integrated Combustion Engine Piston Using Fea Method (CAETools)", *Acta Mechanica Malaysia*, vol. 2, no. 1, pp. 1-5, 2019.
- [7] Z. Wu, W. Dai, M. Man, and E. Luo, "A solar-powered traveling-wave thermoacoustic electricity generator," *Solar Energy* vol. 86, pp. 2376, 2012.
- [8] J. A. Adeff and T. J. Hofler, "Design and construction of a solar-powered, thermoacoustically driven thermoacoustic refrigerator," *J. Acoust. Soc. Am.* vol. 107, no. 6, pp. 37, 2000.
- [9] H. Yan, B. Zhang, "The Practice of Environmental Cost Management of Hydrologic Chemistry in Japan and Its Reference to China", *Advances In Industrial Engineering And Management*, vol. 8, no. 1, pp. 67-69, 2019.
- [10] S. Sakamoto, T. Tsujimoto, and Y. Watanabe, "Generation mechanism of heat flows near the Stack as a prime mover in athermoacoustic cooling system," *Jpn. J. Appl. Phys.* 43, 2751, 2004.
- [11] M. E. Poese, R. W. M. Smith, S. L. Garrett, R. Gerwen, and P. Gosselin, "Thermoacoustic refrigeration for ice cream sales," *Proc. Sixth IIR Gustav Lorentzen Conference*, 2004.
- [12] G. Nazir, S. Gul, "Comparative Study Of Mathematical Model Of Ebola Virus Disease Via Using Differential Transform Method And Variation Of Iteration Method", *Matrix Science Mathematic*, vol. 3, no. 1, pp. 17-19, 2019.
- [13] M. E. H. Tijani and S. Spoelstra, "Study of a coaxial thermoacoustic-Stirling cooler," *Cryogenics* 48, pp.77-82, 2008.
- [14] G. Takeuchi, S. Sakamoto, and Y. Watanabe, "Effect of inner tube diameter on a coaxial thermoacoustic engine," *Proceedings of Symposium on Ultrasonics*, vol. 3 pp. 465-466, 2014.
- [15] Y. Takeyama, S. Sakamoto, and Y. Watanabe, "Study on the setting position of a prime mover in the coaxial-type thermoacoustic cooling system: Comparison with the straight-tube-type thermoacoustic system," *Jpn. J. Appl. Phys.* vol.57 No. 7S1 07LE14, 2018.
- [16] N. Rott, "Damped and thermally driven acoustic oscillations in wide and narrow tubes," *Z. Angew. Math. Phys.* vol.20, pp.230-243, 1969.